Published in final edited form as:
Nat Neurosci. 2010 July ; 13(7): 838–844. doi:10.1038/nn.2576.

Developmental shift to a mechanism of synaptic vesicle endocytosis requiring nanodomain Ca^{2+}

Takayuki Yamashita[1], **Kohgaku Eguchi**[1], **Naoto Saitoh**[2], **Henrique von Gersdorff**[3], and **Tomoyuki Takahashi**[1,2]

[1]Cellular & Molecular Synaptic Function Unit, Initial Research Project, Okinawa Institute of Science and Technology Promotion Corporation, Okinawa, Japan

[2]Department of Neurophysiology, Doshisha University Faculty of Life and Medical Sciences, Kyoto, Japan

[3]The Vollum Institute, Oregon Health and Science University, Portland, Oregon, USA

Abstract

Ca^{2+} is thought to be essential for the exocytosis and endocytosis of synaptic vesicles. However, the manner in which Ca^{2+} coordinates these processes remains unclear, particularly at mature synapses. Using membrane capacitance measurements from calyx of Held nerve terminals in rats, we found that vesicle endocytosis is initiated primarily in Ca^{2+} nanodomains around Ca^{2+} channels, where exocytosis is triggered. Bulk Ca^{2+} outside of the domain could also be involved in endocytosis at immature synapses, although only after extensive exocytosis at more mature synapses. This bulk Ca^{2+}-dependent endocytosis required calmodulin and calcineurin activation at immature synapses, but not at more mature synapses. Similarly, GTP-independent endocytosis, which occurred after extensive exocytosis at immature synapses, became negligible after maturation. We propose that nanodomain Ca^{2+} simultaneously triggers exocytosis and endocytosis of synaptic vesicles and that the molecular mechanisms underlying Ca^{2+}-dependent endocytosis undergo major developmental changes at this fast central synapse.

On arrival of an action potential at a nerve terminal, Ca^{2+} enters through voltage-gated Ca^{2+} channels and forms a high intracellular Ca^{2+} concentration ($[Ca^{2+}]_i$) domain of tens (nanodomain) to hundreds (microdomain) of nanometers in diameter. Ca^{2+} in this domain triggers the fusion of synaptic vesicles with the plasma membrane for exocytic neurotransmitter release. Fused vesicle membrane is subsequently re-internalized by endocytosis and recycled[1,2] into the vesicle pool to be reused for synaptic transmission. Although the critical role of intracellular Ca^{2+} in exocytosis is well established, its role in endocytosis remains less certain. In secretory cells[3] and at synapses[4-6], intracellular Ca^{2+} is involved in fast vesicle endocytosis having a time constant of subseconds to seconds. At the auditory calyx of Held synapse in immature rats, slow endocytosis, having a time constant of tens of seconds, depends on intracellular Ca^{2+}, with the endocytic rate being faster at

Correspondence should be addressed to T.T. (ttakahas@mail.doshisha.ac.jp) or T.Y. (tyamashi@oist.jp).

AUTHOR CONTRIBUTIONS

T.Y. and T.T. designed the experiments. H.v.G. designed the experiments on nonhydrolysable GTP analogues. T.Y., K.E. and N.S. performed the experiments and analyzed the data. T.Y., H.v.G. and T.T. wrote the manuscript. All of authors revised and approved the final manuscript.

Note: Supplementary information is available on the Nature Neuroscience website.

COMPETING FINANCIAL INTERESTS

The authors declare no competing financial interests.

higher $[Ca^{2+}]_i$[7,8]. However, at more mature calyces[9] or at cultured hippocampal synapses[10,11], endocytic rate is relatively constant for various magnitudes of Ca^{2+} influx and exocytosis.

The Ca^{2+} chelators EGTA and BAPTA have similar Ca^{2+}-binding affinities, but BAPTA has a more than hundred-fold faster Ca^{2+}-binding rate than EGTA[12]. These Ca^{2+} buffers are often used for assessing the distance from Ca^{2+} source to its sensor[13]. At immature calyces of Held, before hearing onset (postnatal day 10–12, P10–12)[14], EGTA loaded into the terminal strongly reduces transmitter release[15]. After rodents start to hear sound, however, the inhibitory effect of EGTA becomes much weaker, whereas that of BAPTA is unchanged[16], suggesting that the domains, where Ca^{2+}-secretion coupling occurs, undergo developmental reduction in diameter from microdomain to nanodomain. At immature calyces, similar to vesicle exocytosis, endocytosis is also attenuated by EGTA when loaded into the terminal[7,8], suggesting the involvement of bulk $[Ca^{2+}]_i$ elevation that extends to outside of the nanodomain in vesicle endocytosis. However, the question as to whether $[Ca^{2+}]_i$ in the nanodomain affects vesicle endocytosis remains open, especially at more mature synapses.

Another question of vesicle endocytosis is what is the molecular mechanism downstream of Ca^{2+}. In chromaffin cells[17] and at immature calyces of Held[8], calmodulin (CaM) is thought to mediate Ca^{2+}-dependent vesicle endocytosis. Furthermore, in chromaffin cells[18,19] and brain synaptosomes[20], the Ca^{2+}/CaM-dependent protein phosphatase calcineurin (CaN) is thought to underlie endocytosis via dephoshorylation of a group of endocytic proteins[21], which promotes their assemblies[22]. Vesicle endocytosis generally depends on GTP hydrolysis[23,24], but GTP-independent endocytosis has also been reported at retinal bipolar terminals[25] and immature calyces of Held[26]. We asked whether these endocytic mechanisms operate at the calyx of Held after hearing onset. Our results indicate that nanodomain Ca^{2+} is involved in the fast and slow modes of vesicle endocytosis, both of which are independent of CaM/CaN, but entirely dependent on GTP hydrolysis at the calyx of Held after hearing onset.

RESULTS

Effects of Ca^{2+} buffers on vesicle endocytosis

At the calyx of Held presynaptic terminal of rats before (P7–9, pre-hearing) and after (P13–14, post-hearing) hearing onset, we elicited exocytosis using Ca^{2+} currents induced by a 20-ms square depolarizing pulse (from −80 to +10 mV) and recorded the exocytic increase in membrane capacitance (C_m) followed by a slow endocytic C_m decrease[6-9,23]. The endocytic C_m decay time course decreased as the rats aged[9] (time constant, $\tau = 30.3 \pm 4.2$ s ($n = 8$) at P7–9 and 17.8 ± 1.2 s ($n = 9$) at P13–14, $P < 0.05$; Fig. 1). To examine whether intracellular Ca^{2+} is involved in such slow endocytosis, we first loaded the slow Ca^{2+} chelator EGTA at 10 mM into calyceal terminals via whole-cell patch pipettes. EGTA slowed the endocytic C_m decay at P7–9 calyces (Fig. 1a,b), as previously reported[7,8], but had no effect at P13–14 (Fig. 1c,d). The fast Ca^{2+} chelator BAPTA loaded at 1 mM also slowed endocytosis to a greater extent than 10 mM EGTA at P7–9 calyces[7]. However, 1 mM BAPTA had no effect at P13–14 (Fig. 1d). At pre-hearing calyces, the rate of endocytosis becomes slower as the amount of exocytosis becomes larger[6,7,9,23], whereas at P13–14, the endocytic τ was constant when evoked by a short (1–20 ms) depolarizing pulse (Supplementary Fig. 1)[9]. Thus, the lack of effect of 10 mM EGTA and 1 mM BAPTA on endocytic rate at post-hearing calyces would not be secondary to their inhibitory effects on exocytosis.

Might endocytosis at mature synapses be independent of Ca^{2+} or dependent exclusively on a transient increase of $[Ca^{2+}]_i$ in Ca^{2+} nanodomains, which cannot be attenuated by 10 mM

EGTA or 1 mM BAPTA[12,13]? To investigate this issue, we loaded P13–14 calyces with 10 mM BAPTA. Exocytosis evoked by single 20-ms depolarizing pulse was abolished by 10 mM BAPTA (data not shown), so we evoked a larger exocytosis using a short (1 s) train of repetitive depolarizing pulses (20 times at 20 Hz; Fig. 1e). This train induced a larger exocytic C_m change (ΔC_m, 1.33 ± 0.11 pF, $n = 9$) followed by a bi-exponential endocytic C_m decay (τ_{fast} = 1.5 ± 0.3 s, 39 ± 5%, τ_{slow} = 14.9 ± 2.8 s, τ_{mean} = 9.9 ± 1.9 s, $n = 9$), which was slightly slowed by 10 mM EGTA (τ_{mean} = 17.7 ± 3.1 s, $n = 8$, $P = 0.031$; Fig. 1e,f). After loading with 10 mM BAPTA, exocytic ΔC_m was strongly reduced, but a small exocytic fraction remained (0.20 ± 0.02 pF, $n = 5$). Notably, this exocytosis was not followed by an endocytic C_m decay (Fig. 1e,f). Thus, 10 mM BAPTA completely abolished endocytosis at more mature calyces. These results suggest that vesicle endocytosis after exocytosis is triggered primarily by nanodomain Ca^{2+} at post-hearing nerve terminals.

Ca^{2+}-dependent fast and slow endocytosis

We next investigated the mechanisms underlying fast and slow endocytosis induced by repetitive stimulation[6] (Fig. 2). When the calyx of Held terminal in P7–9 rats was repetitively stimulated by 20-ms depolarizing pulses at 1 Hz, C_m increases summed, and concomitantly the endocytic C_m decay after each pulse (initial rate, 41 ± 7 fF s^{-1}, $n = 16$) became gradually faster and reached a maximal rate ($rate_{max}$) at around the eighth pulse (Fig. 2a) of 160 ± 11 fF s^{-1} (mean value of 10^{th}–20^{th} events; Fig. 2b). In P13–14 calyces, the 1-Hz train also induced endocytic acceleration (Fig. 2d) and reached a $rate_{max}$ (207 ± 32 fF s^{-1}, $n = 8$; Fig. 2a) similar to that at P7–9 ($P = 0.2$). After the 1-Hz train, C_m slowly recovered to the baseline, with a τ_{mean} of 38.8 ± 5.6 s ($n = 7$) at P7–9 (Fig. 2a,c) and 21.6 ± 0.9 s ($n = 7$) at P13–14 (Fig. 2d,f). Thus, the endocytic rate after repetitive stimulation became faster as the rats aged ($P = 0.021$).

To examine the Ca^{2+} dependence of endocytosis induced by this stimulation protocol, we loaded EGTA (10 mM) into the calyceal terminals. In P7–9 calyces, EGTA potently inhibited the endocytic acceleration during the stimulus train as previously reported[6], with its $rate_{max}$ being reduced to 27.1 ± 4.8 fF s^{-1} ($n = 6$, $P < 0.0001$; Fig. 2a,b). In P13–14 calyces, EGTA also attenuated the endocytic acceleration (Fig. 2d,e), but to a lesser extent than in P7–9 calyces ($rate_{max}$, 87.2 ± 9.6 fF s^{-1}, $n = 9$). Essentially the same results were obtained for the percentage of C_m recovery during the 1-Hz pulse (Supplementary Fig. 2). In both age groups, the slow C_m recovery after the stimulus train was inhibited by 10 mM EGTA, with its effect being weaker in post-hearing calyces (Fig. 2). Thus, bulk $[Ca^{2+}]_i$ elevation contributed to both fast and slow types of endocytosis and its contribution decreased as the rats matured. In P13–14 calyces, 10 mM BAPTA nearly abolished the EGTA-resistant endocytosis during and after the repetitive stimulation (Fig. 2d–f), suggesting that nanodomain Ca^{2+} is primarily involved in endocytosis with different kinetics at post-hearing calyceal terminals.

CaM/CaN-dependent endocytosis at immature terminals

These results suggest that both the fast and slow modes of endocytosis can be triggered by intracellular Ca^{2+} at both pre-hearing and post-hearing calyces of Held. At pre-hearing calyces, it has recently been reported that CaM initiates all forms of endocytosis[8]. We re-examined this issue in pre-hearing and post-hearing calyces with intraterminal loadings of the CaM-specific inhibitors, myosin light-chain kinase (MLCK) peptide or CaM-binding domain (CBD) peptide. At pre-hearing calyces, MLCK peptide (0.2 μM) significantly attenuated endocytic acceleration during the 1-Hz stimulation (Fig. 3a,b) and reduced the $rate_{max}$ (81.3 ± 13 fF s^{-1}, $n = 6$) compared with the control peptide (0.2 μM), which cannot bind to CaM[27] (194.6 ± 20.8 fF s^{-1}, $P < 0.01$). MLCK peptide at a higher concentration (30 μM) had a similar inhibitory effect ($rate_{max}$ = 83.8 ± 14 fF s^{-1}, $n = 7$), suggesting that its

maximal effect was attained at 0.2 μM. CBD peptide (20 μM) also reduced the $rate_{max}$ (Fig. 3a,b) to 70.4 ± 9.1 fF s^{-1} (n = 5). In addition to its effect on fast endocytosis, MLCK peptide (0.2 μM) significantly prolonged the slow endocytosis after the 1-Hz train, with its half decay time ($\tau_{0.5}$, 58.1 ± 8.0 s, n = 5) being longer than that observed after control peptide loading (21.1 ± 1.1 s, n = 5, P < 0.01; Fig. 3a,c). CBD peptide (20 μM) showed a similar inhibitory effect on the slow endocytosis ($\tau_{0.5}$ = 55.5 ± 8.7 s, n = 5; Fig. 3a,c). These results confirm that CaM activity is involved in Ca^{2+}-dependent fast and slow endocytosis at pre-hearing calyceal synapses[8].

To determine whether CaM-dependent endocytosis depends on nanodomain Ca^{2+}, we loaded calyces with 10 mM EGTA, together with MLCK peptide (0.2 μM). In the presence of 10 mM EGTA, MLCK peptide had no further inhibitory effect on endocytosis evoked by the 1-Hz train (Fig. 3a,c). Thus, elevation of bulk $[Ca^{2+}]_i$ is required for activation of CaM mediating fast and slow endocytosis.

We next examined whether CaN might mediate the CaM-dependent endocytic components by loading either the CaN inhibitor FK-506 (0.1 μM) or cyclosporin A (CysA, 1 μM) into P7–9 rat calyces. Similar to the CaM inhibitors, these CaN inhibitors attenuated the endocytic acceleration, reducing the $rate_{max}$ attained during the stimulus train (control, 194.5 ± 20.4 fF s^{-1}, n = 11; FK-506, 103.0 ± 9.1 fF s^{-1}, n = 11, P < 0.01; CysA, 110.8 ± 10.2 fF s^{-1}, n = 8, P < 0.01; Fig. 3d,e). The CaN inhibitors also slowed endocytic C_m decay after the 1-Hz train with increased $\tau_{0.5}$ (control, 19.7 ± 2.4 s, n = 7; FK-506, 55.8 ± 9.0 s, n = 6, P < 0.01; CysA, 51.0 ± 5.0 s, n = 6, P < 0.01; Fig. 3d,f). Loading FK-506 or CysA at a higher concentration (10 μM) had no additional effect (data not shown), suggesting that the maximal effect was attained by FK-506 at 0.1 μM and CysA at 1 μM. When we loaded both FK-506 (0.1 μM) and MLCK peptide (0.2 μM), their combined effects on fast and slow endocytosis were not stronger than their individual effects (Fig. 3d–f), suggesting that CaN exclusively mediates the downstream effect of CaM on vesicle endocytosis. Thus, the Ca^{2+}-CaM-CaN cascade mediates a large fraction of fast and slow endocytosis during and after repetitive stimulation at pre-hearing calyces of Held.

Developmental decline of the CaM/CaN-dependent endocytosis

We next examined whether the Ca^{2+}-CaM-CaN–dependent endocytic mechanism persists in the post-hearing calyces of Held by loading either MLCK peptide (30 μM) or CBD peptide (20 μM) into P13–14 calyces. In contrast with pre-hearing calyces, these CaM inhibitor peptides no longer affected endocytosis during or after the 1-Hz train at P13–14 (Fig. 4a–c and Supplementary Fig. 3). Similarly, the CaN inhibitors FK-506 (10 μM) and CysA (10 μM) no longer affected endocytosis evoked by the stimulus train at P13–14 calyces (Fig. 4d–f). These results suggest that neither fast nor slow endocytosis is mediated by the Ca^{2+}-CaM-CaN cascade at the calyx of Held after hearing onset.

What developmental change causes the loss of functions of CaM and CaN in endocytosis? During the second postnatal week, CaM expression at calyceal terminals remains unchanged[28]. We therefore examined the expression of CaN in pre-hearing and post-hearing calyces. Immuno-staining with antibody to CaN (Fig. 5a) revealed that CaN was universally expressed at calyceal terminals in P7–8 rats, which were identified by synaptophysin immunoreactivity. At calyces in P14–15 rats, however, CaN immunoreactivity was much weaker (Fig. 5a). In densitometric quantification after subtracting the background in the presence of exogenous CaN, the intensity of CaN immunoreactivity at P14–15 calyces was 61% of that at P7–8 (Fig. 5b). Consistently, western blot analysis using tissue samples from the medial nucleus of trapezoid body (MNTB) regions also revealed a significant developmental decrease (to 66%, from P7 to P14, P = 0.04) in CaN immunoreactivity (Supplementary Fig. 4). Thus, CaN expression at the calyceal terminals was apparently

downregulated during development, which may contribute, at least in part, to the developmental decline of the involvement of the Ca^{2+}-CaM-CaN cascade in vesicle endocytosis.

GTP dependence of endocytosis at the calyx of Held

At pre-hearing calyces (P7–9), the nonhydrolysable GTP analog GTPγS nearly abolishes slow endocytosis induced by a single depolarizing pulse (duration, 1–20 ms) when loaded into the terminal at 0.2–0.3 mM[23,26]. However, a more recent study reported the presence of GTPγS-resistant endocytosis, which became apparent as the net exocytic C_m increases by more than 2 pF during intensive stimulation[26]. At the retinal bipolar cell terminal, GTPγS has no effect on endocytosis at 3.5 mM[25], but abolishes it at 5 mM[24]. We therefore asked whether vesicle endocytosis can be observed in the presence of 5 mM GTPγS (tetralithium salt) at pre-hearing calyces. To minimize GTP synthesis from ATP, we removed the ATP-generating reagent phosphocreatine and reduced the ATP concentration to 2 mM in the pipette solution. In this condition, small fractions of fast and slow endocytosis were discerned during and after the 1-Hz train (Fig. 6a–c), confirming a previous report[26]. To determine whether this GTPγS-resistant component is CaM dependent or not, we loaded MLCK peptide (0.2 μM) and GTPγS (5 mM) into P7–9 calyces. In the presence of GTPγS, MLCK peptide had no additional effect on endocytosis during or after the 1-Hz train (Fig. 6a–c), indicating that GTPγS occluded the inhibitory effect of MLCK peptide on vesicle endocytosis. Thus, at immature calyces, the GTP-independent minor endocytic component was not mediated by CaM and the CaM-dependent fast and slow endocytosis was entirely GTP dependent.

We next examined whether this GTP-independent endocytosis persists after hearing onset. In P13–14 calyces, GTPγS (5 mM) completely abolished endocytosis during and after the 1-Hz train, despite the fact that the exocytic ΔC_m accumulated during the train (3.4 ± 0.3 pF, n = 8) was greater than that at pre-hearing calyces (P = 0.043) (Fig. 6d–f). Thus, vesicle endocytosis appears to become entirely GTP dependent during the second postnatal week at the calyx of Held.

DISCUSSION

Nanodomain Ca^{2+} couples endocytosis to exocytosis

To maintain transmitter release by vesicle recycling and to keep the area of presynaptic membrane constant, the amount of vesicle exocytosis must be somehow reported to the endocytic machinery. It has been suggested that Ca^{2+} does this in the case of massive exocytosis[4-7]. Our results suggest that Ca^{2+} acts, also for moderate exocytosis in a physiological range, by simultaneously triggering both exocytosis and endocytosis of synaptic vesicles in the Ca^{2+} nanodomain at relatively mature calyces of Held. This is consistent with endocytic rate not being dependent on stimulus intensity over a wide range at relatively mature synapses[9-11] (Supplementary Fig. 1). In response to an action potential, [Ca^{2+}] in the nanodomain (within 50 nm of Ca^{2+} channels[13]) rises to hundreds of micromolar and dissipates in milliseconds[29], thereby triggering exocytic transmitter release[16]. During such a short period, Ca^{2+} may prime vesicles for endocytosis, which occurs after exocytosis over tens of seconds and is not Ca^{2+} dependent[30], possibly at the peri-active zone[31,32]. The actual distance between the sites of Ca^{2+} entry and vesicle endocytosis remains unknown.

Simultaneous activation of exocytic and endocytic machineries by nanodomain Ca^{2+} would allow low-affinity Ca^{2+}-binding proteins such as synaptotagmin[33,34] and synaptophysin[35] to be involved in endocytosis, supporting the idea that these proteins have dual roles in vesicle

exocytosis and endocytosis. This is also consistent with the hypothesis that the C terminus[36] or synprint site[37] of the α subunit of voltage-gated Ca^{2+} channel is involved in vesicle endocytosis via its direct interaction with endocytic proteins. On prolonged repetitive stimulation, Ca^{2+} would spill out of the nanodomain. In such a condition, bulk Ca^{2+} would become involved in vesicle endocytosis to prevent the nerve terminal from aberrant swellings and from severe synaptic vesicle pool depletion.

Developmental changes in endocytic mechanisms

Consistent with previous studies in secretory cells[3] and nerve terminals[4-8], our results indicate that bulk Ca^{2+} that accumulates outside of the Ca^{2+} nanodomain contributes to fast and slow endocytosis at the pre-hearing and post-hearing calyces. The CaM-CaN–signaling mechanism was downstream of bulk Ca^{2+} at pre-hearing calyces, as in secretory cells[18,19] and synaptosomes[20]. However, this mechanism no longer operated after hearing onset. Similarly, Ca^{2+} and CaM underlie inactivation of presynaptic Ca^{2+} currents[28,38] at pre-hearing calyces of Held, but not at post-hearing calyces[28], presumably as a result of a developmental decline in residual bulk $[Ca^{2+}]_i$[39] below the threshold for CaM activation (K_d, 2–9 μM)[40]. This developmental change, together with the downregulation of CaN expression, might explain the lack of CaM- and CaN-dependent endocytosis in the post-hearing calyces. Although NCS-1 family, CaBP1 and hippocalcin have a Ca^{2+}-binding affinity that is 1–2 orders of magnitude higher than CaM[41], it remains to be seen whether these Ca^{2+}-binding proteins might be involved in vesicle endocytosis at mature synapses with lower bulk $[Ca^{2+}]_i$.

Another controversial issue of vesicle endocytosis is its GTP dependence. Although we confirmed the presence of the GTP-independent endocytosis at pre-hearing calyces[26], as has been seen at retinal bipolar terminals[25], this mechanism no longer operated after hearing onset. Similarly, at the neuromuscular synapse in *Drosophila*, some forms of short-term depression do not depend on dynamin GTPase at the larval stage[42], but there is an acute need for dynamin during repetitive stimulation at mature synapses[43] and the synaptic vesicle pool is severely depleted in dynamin-deficient flies[2]. Dynamin 1 is essential for the slow mode of endocytosis after strong stimuli[44], and pretreatment of synapses with dynamin inhibitors blocks synaptic transmission after prolonged repetitive stimulation[23,45]. Thus, a GTP- and dynamin-dependent form of endocytosis may be critical for mature synapses to properly function.

Vesicle endocytosis is typically classified into fast and slow modes[46,47], whose relative prominence depends on Ca^{2+} buffer type and concentration[4,7,8]. However, our results suggest that this classification does not agree with underlying mechanisms. At post-hearing calyces, 10 mM EGTA had no effect on slow endocytosis lasting tens of seconds following a short pulse (20 ms) stimulation, whereas it attenuated endocytosis with similar kinetics following a repetitive stimulation. The remaining EGTA-resistant endocytic components were abolished by 10 mM BAPTA. These results suggest that slow endocytosis can be mediated by distinct Ca^{2+} sensors residing inside and outside of the Ca^{2+} nanodomain. At pre-hearing calyces, fast endocytosis during a repetitive stimulus and slow endocytosis after the train had similar pharmacological properties, with both being sensitive to 10 mM EGTA and inhibitors for CaM and CaN. Thus, endocytosis with different kinetics can be mediated by a common mechanism. Fast endocytosis during the repetitive stimulation had a similar kinetics throughout P7–14, but the underlying mechanism was independent of CaM and CaN after hearing onset. Thus, a classification from a more mechanistic viewpoint remains to be established for vesicle endocytosis with different kinetics.

ONLINE METHODS

Slice preparation and solutions

All experiments were performed in accordance with the guidelines of the Physiological Society of Japan. Methods for preparing auditory brainstem slices containing the MNTB from Wistar rats (P7–15) have been described previously[23,28]. The extracellular solution for recordings that isolates Ca^{2+} currents contained 115 mM NaCl, 2.5 mM KCl, 26 mM $NaHCO_3$, 1.25 mM NaH_2PO_4, 2 mM $CaCl_2$, 1 mM $MgCl_2$, 10 mM glucose, 3 mM myoinositol, 2 mM sodium pyruvate, 0.5 mM ascorbic acid, 10 mM tetraethyl-ammonium chloride, 0.5 mM 4-aminopyridine, 0.001 mM tetrodotoxin, 0.01 mM bicuculline methiodide and 0.0005 mM strychnine hydrochloride (pH 7.4 when bubbled with 95% O_2 and 5% CO_2, 310–315 mOsm). Unless otherwise noted, the pipette solution contained 118 mM cesium gluconate, 30 mM CsCl, 10 mM HEPES, 0.5 mM EGTA, 1 mM $MgCl_2$, 12 mM sodium phosphocreatine, 3 mM Mg-ATP and 0.3 mM Na-GTP (pH 7.3–7.4 adjusted with CsOH). When we used different concentrations of Ca^{2+} buffers, the osmolarity of the pipette solution was set to 315–320 mOsm by changing the concentration of cesium gluconate. For blocking GTP hydrolysis in the calyceal terminals, we used a modified low-[ATP] pipette solution that contained 128 mM cesium gluconate, 30 mM CsCl, 10 mM HEPES, 0.5 mM EGTA, 1 mM $MgCl_2$, 2 mM Mg-ATP and 5 mM GTPγS (tetralithium salt) (pH 7.3–7.4 adjusted with CsOH). For control experiments using the low-[ATP] pipette solution, CsCl (20 mM) was replaced by equimolar LiCl, GTPγS was omitted and 1 mM Na-GTP was added. GTPγS was stored as powder at −20 °C and dissolved in the pipette solution less than 2 h before recordings.

Recordings and data analysis

C_m measurement from the calyx of Held nerve terminals in whole-cell configurations were made at 26–27 °C as described previously[23]. Calyceal terminals were voltage clamped at the holding potential of −80 mV and the sinusoidal voltage command was applied at 1 kHz with a peak-to-peak voltage of 60 mV. Patch pipettes (5–8 MΩ) had a series resistance of 7–20 MΩ, which was compensated by up to 65% for a final value of 6.7–7.0 MΩ. The pipettes were coated with dental wax to reduce stray capacitance (4–6 pF, compensated by >80%). Data were obtained within 20 min of break-in. Single pulse or a train (1 Hz) of step depolarization (to +10 mV, 20 ms) was used for stimulation, unless otherwise noted. C_m changes within 450 ms of square-pulse stimulation were excluded from analysis to avoid contaminations of conductance-dependent capacitance artifacts[23]. The amplitude of exocytic C_m change (ΔC_m) was measured as the difference of C_m values between the baseline and at 450–500 ms after depolarization. For measuring C_m decay rate during repetitive stimulation at 1 Hz, regression lines were obtained from C_m records 0.45–1 s after each pulse. Sample C_m records are shown as average values of each 50 data point (for 50 ms) plotted every 50 ms (for shorter time scale) or every 500 ms (for longer time scale). GTPγS, LiCl, DMSO, MLCK peptide (RRKWQKTGHAVRAIGRL, Calbiochem), MLCK two-point mutant peptide[27] (control peptide, RRKEQKTGHAVRAIGRE, Calbiochem), CBD peptide (CaM kinase II 290–309, Sigma), FK-506 (Sigma) and CysA (Tocris Bioscience) were included in the pipette solution and were infused into the calyceal terminals with the access resistance less than 12 MΩ and were allowed to diffuse in the terminals for at least 5 min before recordings. All values are given as mean ± s.e.m. and significant difference was evaluated by one-way ANOVA followed by Dunnett's *post hoc* test or Student's unpaired *t* test, unless otherwise noted.

Immunostaining and immunoblotting

Immunostaining and immunoblotting were performed as previously described[48]. For immunostaining, we used primary antibody to CaN β subunit (mouse monoclonal clone CN-

B1, Sigma, diluted 1:2,000) and primary antibody to synaptophysin (rabbit polyclonal, Zymed Laboratories, diluted 1:100), along with goat secondary antibodies conjugated with Alexa fluor 488 and Alexa fluor 588 (Invitrogen, diluted 1:200). In the primary antibody absorbing tests for evaluating the specificity of the CaN immunoreactivity, bovine brain CaN (Sigma; final concentration, 500 units per ml) was pre-incubated with primary antibodies overnight at 4 °C. Primary antibody dilution buffer (pH 7.3) contained 40 mM HEPES, 300 mM NaCl, 0.2% bovine serum albumin (wt/vol) and 0.05% Triton X-100 (vol/vol). Confocal images were acquired using the Olympus FV300 system with an inverted microscope (IX71) attached with a 60× objective lens (PlanApo) and analyzed using WinROOF software (Mitani). For immunoblotting, the homogenate (2 μg) of tissue samples from the MNTB region of rat brainstem were separated using Tris-tricine gel (15–20%), electro-blotted to PVDF membrane, blocked with skimmed milk, incubated with antibody to CaN β subunit (diluted 1:2,000) overnight at 4 °C and then with horseradish peroxidase–conjugated antibody to mouse IgG (GE Healthcare, diluted 1:2,000) for 40 min at 20–24 °C and detected with ECL advance (GE Healthcare). Chemiluminescent images were acquired using LAS-1000 system (Fujifilm) and analyzed with MultiGauge software (Fujifilm). To quantify the relative amount of CaN in samples, we simultaneously applied 0.5–3 μg homogenate samples to the same gel and formulated a standard curve for measuring the intensity of CaN immunoreactivity.

Supplementary Material

Refer to Web version on PubMed Central for supplementary material.

Acknowledgments

We thank E. Johnson and S. Takamori for helpful comments. This work was supported by the Core Research for Evolutional Science and Technology of Japan Science and Technology Agency (T.T.), US National Institutes of Health grant EY014043 (H.v.G.) and Grant-in-Aid for Young Scientists from the Japanese Ministry of Education, Culture, Sports, Science and Technology #20700357 (T.Y.).

References

1. Heuser JE, Reese TS. Evidence for recycling of synaptic vesicle membrane during transmitter release at the frog neuromuscular junction. J Cell Biol. 1973; 57:315–344. [PubMed: 4348786]
2. Koenig JH, Ikeda K. Disappearance and reformation of synaptic vesicle membrane upon transmitter release observed under reversible blockage of membrane retrieval. J Neurosci. 1989; 9:3844–3860. [PubMed: 2573698]
3. Artalejo CR, Henley JR, McNiven MA, Palfrey HC. Rapid endocytosis coupled to exocytosis in adrenal chromaffin cells involves Ca^{2+}, GTP and dynamin, but not clathrin. Proc Natl Acad Sci USA. 1995; 92:8328–8332. [PubMed: 7667289]
4. Neves G, Gomis A, Lagnado L. Calcium influx selects the fast mode of endocytosis in the synaptic terminal of retinal bipolar cells. Proc Natl Acad Sci USA. 2001; 98:15282–15287. [PubMed: 11734626]
5. Beutner D, Voets T, Neher E, Moser T. Calcium dependence of exocytosis and endocytosis at the cochlear inner hair cell afferent synapse. Neuron. 2001; 29:681–690. [PubMed: 11301027]
6. Wu W, Xu J, Wu X-S, Wu L-G. Activity-dependent acceleration of endocytosis at a central synapse. J Neurosci. 2005; 25:11676–11683. [PubMed: 16354926]
7. Hosoi N, Holt M, Sakaba T. Calcium-dependence of exo- and endocytotic coupling at a glutamatergic synapse. Neuron. 2009; 63:216–229. [PubMed: 19640480]
8. Wu X-S, et al. Ca^{2+} and calmodulin initiates all forms of endocytosis during depolarization at a nerve terminal. Nat Neurosci. 2009; 12:1003–1010. [PubMed: 19633667]

9. Renden R, von Gersdorff H. Synaptic vesicle endocytosis at a CNS nerve terminal: faster kinetics at physiological temperatures and increased endocytotic capacity during maturation. J Neurophysiol. 2007; 98:3349–3359. [PubMed: 17942618]
10. Granseth B, Odermatt B, Royle SJ, Lagnado L. Clathrin-mediated endocytosis is the dominant mechanism of vesicle retrieval at hippocampal synapses. Neuron. 2006; 51:773–786. [PubMed: 16982422]
11. Balaji J, Armbruster M, Ryan TA. Calcium control of endocytic capacity at a CNS synapse. J Neurosci. 2008; 28:6742–6749. [PubMed: 18579748]
12. Naraghi M, Neher E. Linearized buffered Ca^{2+} diffusion in microdomains and its implications for calculation of [Ca^{2+}] at the mouth of a calcium channel. J Neurosci. 1997; 17:6961–6973. [PubMed: 9278532]
13. Augustine GJ, Santamaria F, Tanaka K. Local calcium signaling in neurons. Neuron. 2003; 40:331–346. [PubMed: 14556712]
14. Jewett DL, Romano MN. Neonatal development of auditory system potentials averaged from the scalp of rat and cat. Brain Res. 1972; 36:101–115. [PubMed: 5008374]
15. Borst JGG, Sakmann B. Calcium influx and transmitter release in a fast CNS synapse. Nature. 1996; 383:431–434. [PubMed: 8837774]
16. Fedchyshyn MJ, Wang L-Y. Developmental transformation of the release modality at the calyx of Held synapse. J Neurosci. 2005; 25:4131–4140. [PubMed: 15843616]
17. Artalejo CR, Elhamdani A, Palfrey HC. Calmodulin is the divalent cation receptor for rapid endocytosis, but not exocytosis, in adrenal chromaffin cells. Neuron. 1996; 16:195–205. [PubMed: 8562084]
18. Engisch KL, Nowycky MC. Compensatory and excess retrieval: two types of endocytosis following single step depolarizations in bovine adrenal chromaffin cells. J Physiol (Lond). 1998; 506:591–608. [PubMed: 9503324]
19. Chan S-A, Smith C. Physiological stimuli evoke two forms of endocytosis in bovine chromaffin cells. J Physiol (Lond). 2001; 537:871–885. [PubMed: 11744761]
20. Marks B, McMahon HT. Calcium triggers calcineurin-dependent synaptic vesicle recycling in mammalian nerve terminals. Curr Biol. 1998; 8:740–749. [PubMed: 9651678]
21. Cousin MA, Robinson PJ. The dephosphins: dephosphorylation by calcineurin triggers synaptic vesicle endocytosis. Trends Neurosci. 2001; 24:659–665. [PubMed: 11672811]
22. Slepnev VI, Ochoa G-C, Butler MH, Grabs D, De Camilli P. Role of phosphorylation in regulation of the assembly of endocytic coat complexes. Science. 1998; 281:821–824. [PubMed: 9694653]
23. Yamashita T, Hige T, Takahashi T. Vesicle endocytosis requires dynamin-dependent GTP hydrolysis at a fast CNS synapse. Science. 2005; 307:124–127. [PubMed: 15637282]
24. Jockusch WJ, Praefcke GJK, McMahon HT, Lagnado L. Clathrin-dependent and clathrin-independent retrieval of synaptic vesicles in retinal bipolar cells. Neuron. 2005; 46:869–878. [PubMed: 15953416]
25. Heidelberger R. ATP is required at an early step in compensatory endocytosis in synaptic terminals. J Neurosci. 2001; 21:6467–6474. [PubMed: 11517235]
26. Xu J, et al. GTP-independent rapid and slow endocytosis at a central synapse. Nat Neurosci. 2008; 11:45–53. [PubMed: 18066059]
27. Török K, et al. Inhibition of calmodulin-activated smooth-muscle myosin light-chain kinase by calmodulin-binding peptides and fluorescent (phosphodiesterase-activating) calmodulin derivatives. Biochemistry. 1998; 37:6188–6198. [PubMed: 9558358]
28. Nakamura T, Yamashita T, Saitoh N, Takahashi T. Developmental changes in calcium/calmodulin-dependent inactivation of calcium currents at the rat calyx of Held. J Physiol (Lond). 2008; 586:2253–2261. [PubMed: 18238813]
29. Neher E. Vesicle pools and Ca^{2+} microdomains: new tools for understanding their roles in neurotransmitter release. Neuron. 1998; 20:389–399. [PubMed: 9539117]
30. Gad H, Löw P, Zotova E, Brodin L, Shupliakov O. Dissociation between Ca^{2+}-triggered synaptic vesicle exocytosis and clathrin-mediated endocytosis at a central synapse. Neuron. 1998; 21:607–616. [PubMed: 9768846]

31. Roos J, Kelly RB. The endocytic machinery in nerve terminals surrounds sites of exocytosis. Curr Biol. 1999; 9:1411–1414. [PubMed: 10607569]
32. Teng H, Wilkinson RS. Clathrin-mediated endocytosis near active zones in snake motor boutons. J Neurosci. 2000; 20:7986–7993. [PubMed: 11050119]
33. Poskanzer KE, Marek KW, Sweeney ST, Davis GW. Synaptotagmin 1 is necessary for compensatory synaptic vesicle endocytosis *in vivo*. Nature. 2003; 426:559–563. [PubMed: 14634669]
34. Llinás RR, Sugimori M, Moran KA, Moreira JE, Fukuda M. Vesicular reuptake inhibition by a synaptotagmin I C2B domain antibody at the squid giant synapse. Proc Natl Acad Sci USA. 2004; 101:17855–17860. [PubMed: 15591349]
35. Daly C, Ziff EB. Ca^{2+}-dependent formation of a dynamin-synaptophysin complex: potential role in synaptic vesicle endocytosis. J Biol Chem. 2002; 277:9010–9015. [PubMed: 11779869]
36. Chen Y, et al. Formation of an endophillin-Ca^{2+} channel complex is critical for clathrin-mediated synaptic vesicle endocytosis. Cell. 2003; 115:37–48. [PubMed: 14532001]
37. Watanabe H, et al. Involvement of Ca^{2+} channel synprint site in synaptic vesicle endocytosis. J Neurosci. 2010; 30:655–660. [PubMed: 20071530]
38. Xu J, Wu L-G. The decrease in the presynaptic calcium current is a major cause of short-term depression at a calyx-type synapse. Neuron. 2005; 46:633–645. [PubMed: 15944131]
39. Nakamura Y, DiGregorio D, Takahashi T. Single action potential–evoked Ca^{2+} transients at the calyx of Held presynaptic terminal. Neurosci Res. 2007; 58:S71.
40. Shifman JM, Choi MH, Mihalas S, Mayo SL, Kennedy MB. Ca^{2+}/calmodulin-dependent protein kinase II (CaMKII) is activated by calmodulin with two bound calciums. Proc Natl Acad Sci USA. 2006; 103:13968–13973. [PubMed: 16966599]
41. Burgoyne RD. Neuronal calcium sensor proteins: generating diversity in neuronal Ca^{2+} signaling. Nat Rev Neurosci. 2007; 8:182–193. [PubMed: 17311005]
42. Kawasaki F, Hazen M, Ordway RW. Fast synaptic fatigue in shibire mutants reveals a rapid requirement for dynamin in synaptic membrane trafficking. Nat Neurosci. 2000; 3:859–860. [PubMed: 10966613]
43. Wu Y, Kawasaki F, Ordway RW. Properties of short-term synaptic depression at larval neuromuscular synapses in wild-type and temperature-sensitive paralytic mutants of *Drosophila*. J Neurophysiol. 2005; 93:2396–2405. [PubMed: 15845998]
44. Lou X, Paradise S, Ferguson SM, De Camilli P. Selective saturation of slow endocytosis at a giant glutamatergic central synapse lacking dynamin 1. Proc Natl Acad Sci USA. 2008; 105:17555–17560. [PubMed: 18987309]
45. Newton AJ, Kirchhausen T, Murthy VN. Inhibition of dynamin completely blocks compensatory synaptic vesicle endocytosis. Proc Natl Acad Sci USA. 2006; 103:17955–17960. [PubMed: 17093049]
46. von Gersdorff H, Matthews G. Inhibition of endocytosis by elevated internal calcium in a synaptic terminal. Nature. 1994; 370:652–655. [PubMed: 8065451]
47. Wu L-G, Ryan TA, Lagnado L. Modes of vesicle retrieval at ribbon synapses, calyx-type synapses and small central synapses. J Neurosci. 2007; 27:11793–11802. [PubMed: 17978015]
48. Kimura M, Saitoh N, Takahashi T. Adenosine A_1 receptor–mediated presynaptic inhibition at the calyx of Held of immature rats. J Physiol (Lond). 2003; 553:415–426. [PubMed: 12963795]

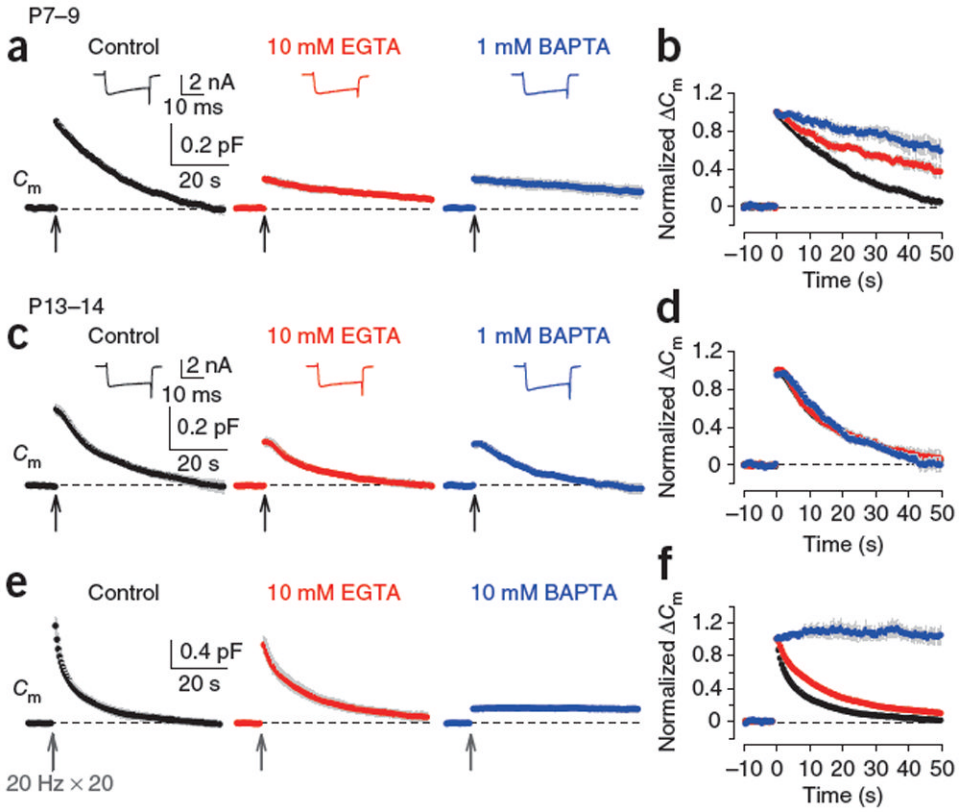

Figure 1.

Different effects of EGTA and BAPTA on vesicle endocytosis at the developing calyces of Held. (**a**) At P7–9 calyceal terminals, presynaptic Ca^{2+} currents (I_{Ca}, upper insets) and C_m changes were evoked by a 20-ms depolarizing command pulse (from −80 to +10 mV, onset is indicated by an arrow) in the presence of 0.5 mM EGTA (control, black), 10 mM EGTA (red) or 1 mM BAPTA (blue) in the whole-cell patch pipette. Average C_m traces from six to eight presynaptic terminals and representative I_{Ca} traces are shown. Gray shading indicates s.e.m. (**b**) C_m traces in **a** normalized at the peak. (**c**) The stimulation protocol described in **a** was applied to P13–14 calyces. Averaged C_m traces were obtained from 5–9 calyceal terminals. (**d**) C_m traces in **c** normalized at the peak. (**e**) C_m changes induced by a train of 20 depolarizing pulses (20-ms duration) at 20 Hz in the presence of 0.5 mM EGTA (control, black, $n = 9$), 10 mM EGTA (red, $n = 8$) or 10 mM BAPTA (blue, $n = 5$) loaded into P13–14 calyces. EGTA (10 mM) had no significant effect on exocytic ΔC_m (1.07 ± 0.10 pF, $P = 0.098$). (**f**) C_m traces in **e** normalized at the peak.

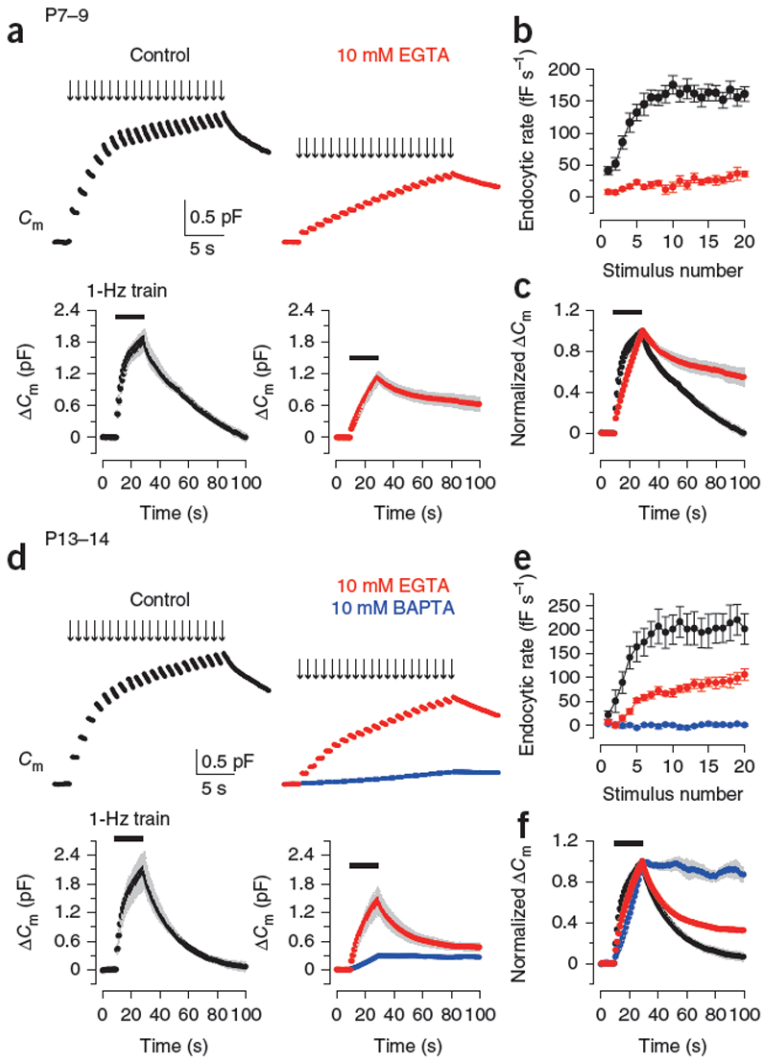

Figure 2.

Ca^{2+} dependence of fast and slow endocytosis elicited by repetitive stimulation at the calyx of Held. (**a**) Top, C_m changes induced by 20-ms depolarizing pulses (arrows indicate onsets) repeated at 1 Hz for 20 s at P7–9 calyceal terminals preloaded with EGTA at 0.5 mM (black, control) or 10 mM (red). Bottom, averaged C_m records, shown at a longer time scale, from P7–9 calyceal terminals with 0.5 mM ($n = 7$) or 10 mM EGTA ($n = 5$). Gray shading indicates s.e.m. Black bars indicate the period of stimulation. (**b**) Endocytic rate during the stimulus train (fF s^{-1}, ordinate), estimated from linear regression line fit to the C_m decay 0.45–1 s after each pulse versus stimulus number (abscissa) in P7–9 calyces with 0.5 mM (black, $n = 16$) or 10 mM EGTA (red, $n = 6$). (**c**) C_m traces from **a** normalized at the peak (superimposed). (**d–f**) Data are presented as in **a–c** for P13–14 calyces ($n = 5–9$). Data from terminals loaded with 10 mM BAPTA (blue) are also shown. Error bars represent s.e.m.

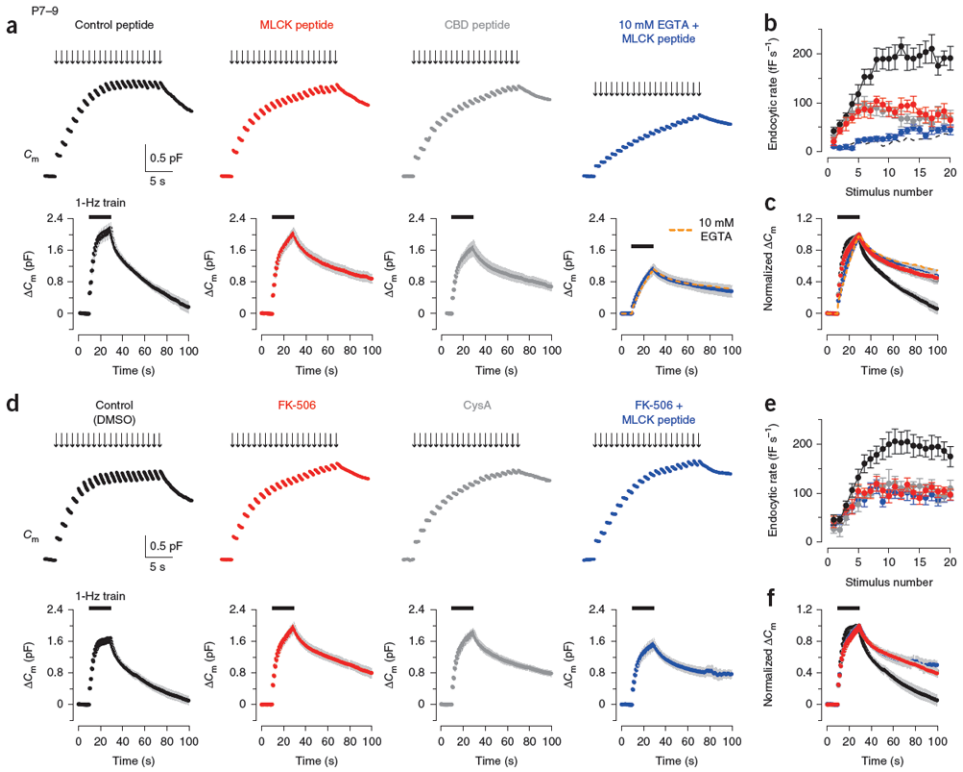

Figure 3.

Effects of inhibitors for CaM and CaN in fast and slow endocytosis at P7–9 calyces. (**a**) Top, C_m changes induced by a stimulus train (20 pulses of 20-ms depolarization at 1 Hz) in the terminal preloaded with control peptide (0.2 μM, black, P8), MLCK peptide (0.2 μM, red, P8), CBD peptide (20 μM, dark gray, P8) or MLCK peptide (0.2 μM) and 10 mM EGTA (blue, P9). Bottom, averaged C_m records, shown at a slow time scale, from P7–9 calyceal terminals ($n = 5$ for each). Data from terminals preloaded with 10 mM EGTA (Fig. 2a) were superimposed (dashed orange line) on data from terminals preloaded with 10 mM EGTA and MLCK peptide (blue) in the bottom right panel. Gray shading indicates s.e.m. Black bars indicate the period of stimulation. (**b**) Summary data for the C_m decay rate (ordinate) measured after each pulse during the 1-Hz train versus stimulus number (abscissa) in the presence of control peptide (black, $n = 6$), MLCK peptide (red, $n = 6$), CBD peptide (dark gray, $n = 5$) or MLCK peptide and 10 mM EGTA (blue, $n = 6$). Dashed line indicates data from 10 mM EGTA-loaded terminals (Fig. 2a). (c) Averaged C_m traces shown in **a** normalized at the peak (superimposed). (**d–f**) Data are presented as in **a–c** for terminals loaded with 0.1% DMSO (black) or calyceal terminals loaded with FK-506 (0.1 μM, with 0.1% DMSO, red), cyclosporin A (CysA, 1 μM, with 0.1% DMSO, dark gray) or FK-506 and MLCK peptide (0.2 μM, blue) in P7–9 rats. Sample records (top panels of **d**) were derived from different calyceal terminals in P8 rats. Averaged C_m records (bottom panels of **d**) were obtained from 6–11 terminals. Error bars represent s.e.m.

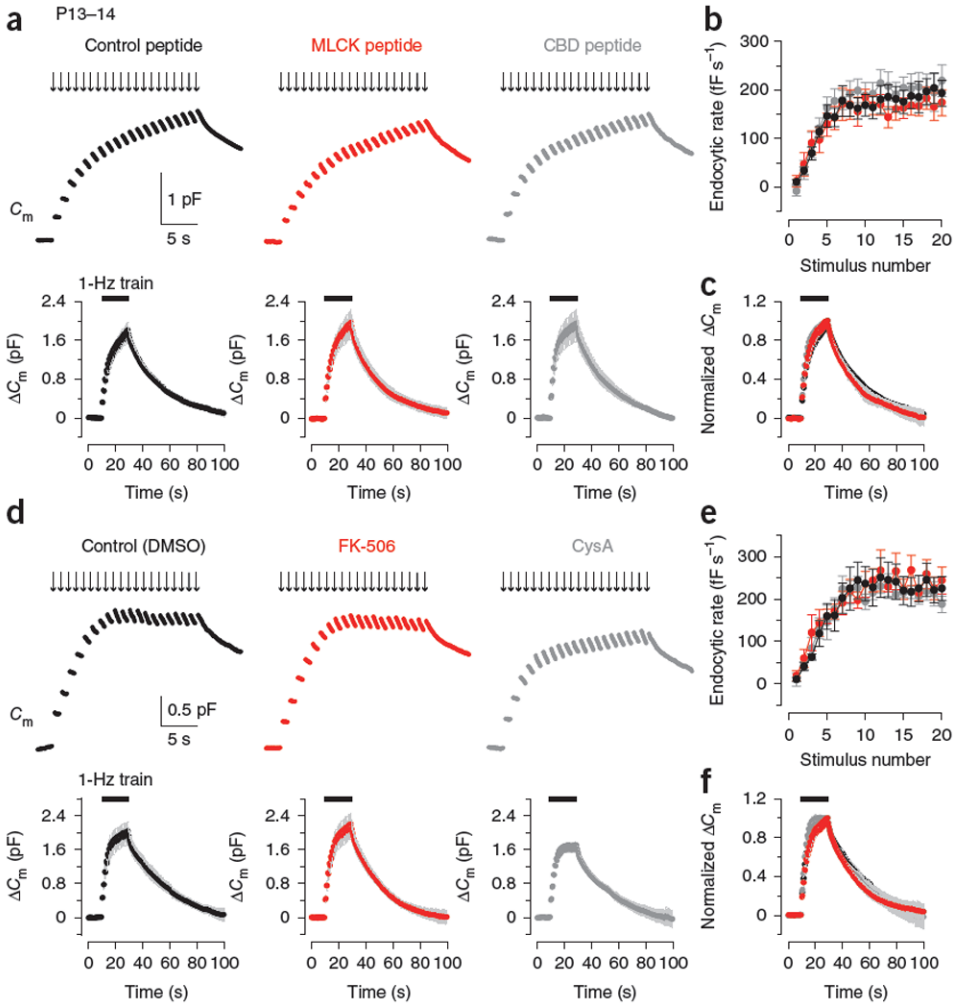

Figure 4.

No effect of inhibitors for CaM and CaN in fast and slow endocytosis at P13–14 calyces. (**a**) Top, sample C_m changes induced by a 1-Hz train of 20 depolarizing pulses with the pipette solution containing control peptide (30 μM, black), MLCK peptide (30 μM, red) or CBD peptide (20 μM, dark gray) at P13–14 calyces. Bottom, averaged C_m records from P13–14 calyces loaded with control peptide (black, $n = 6$), MLCK peptide (red, $n = 8$) or CBD peptide (dark gray, $n = 5$). Gray shading indicates s.e.m. Black bars indicate the period of stimulation. (**b**) Summary data for the C_m decay rate after each pulse during the 1-Hz train from presynaptic terminals loaded with control peptide (black, $n = 6$), MLCK peptide (red, $n = 8$) or CBD peptide (dark gray, $n = 6$). (**c**) Averaged C_m traces from **a** normalized at the peak (superimposed). (**d–f**) Data are presented as in **a–c** for calyces loaded with 0.1% DMSO (control, black), FK-506 (10 μM, with 0.1% DMSO, red) or CysA (10 μM, with 0.1% DMSO, dark gray) in P13–14 rats ($n = 5–6$ terminals). Error bars represent s.e.m.

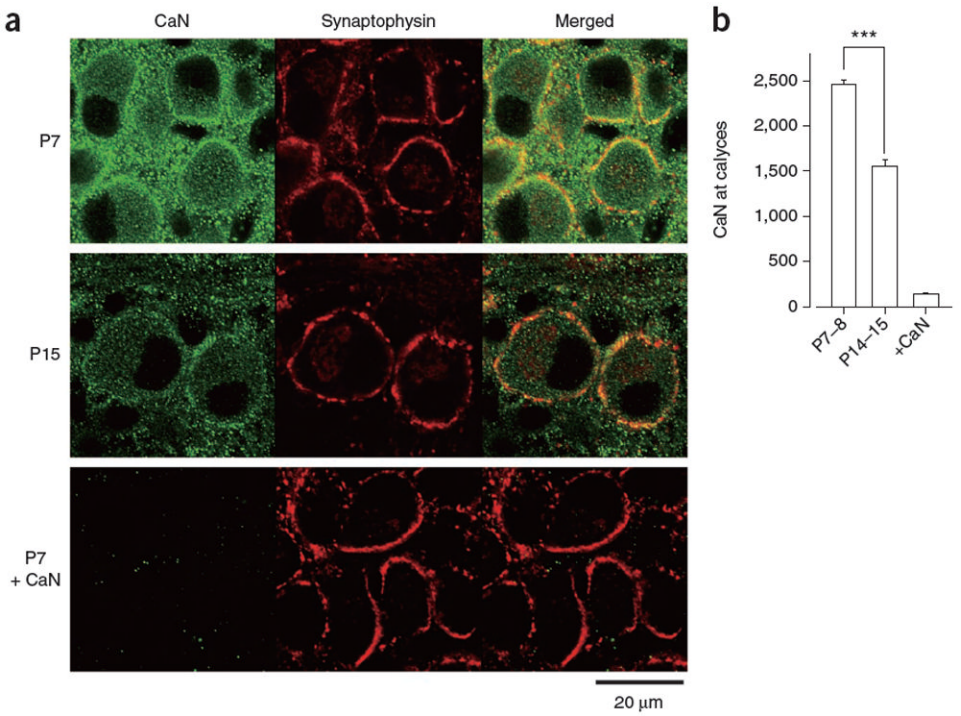

Figure 5.

Developmental decline of CaN expression at the calyx of Held presynaptic terminals. (**a**) CaN immunoreactivity (left, green), synaptophysin immunoreactivity (middle, red) and their overlap (right). Bottom left (P7 + CaN), background after absorbing the primary antibodies with CaN protein. (**b**) Densitometric measurements of CaN immunofluorescence intensity in the regions that overlapped with synaptophysin immunofluorescence signals in P7–8 and P14–15 preparations (***$P < 0.001$, Scheffe test) and the background intensity measured after antibody absorption in P7–P15 preparations (+CaN). Error bars represent s.e.m.

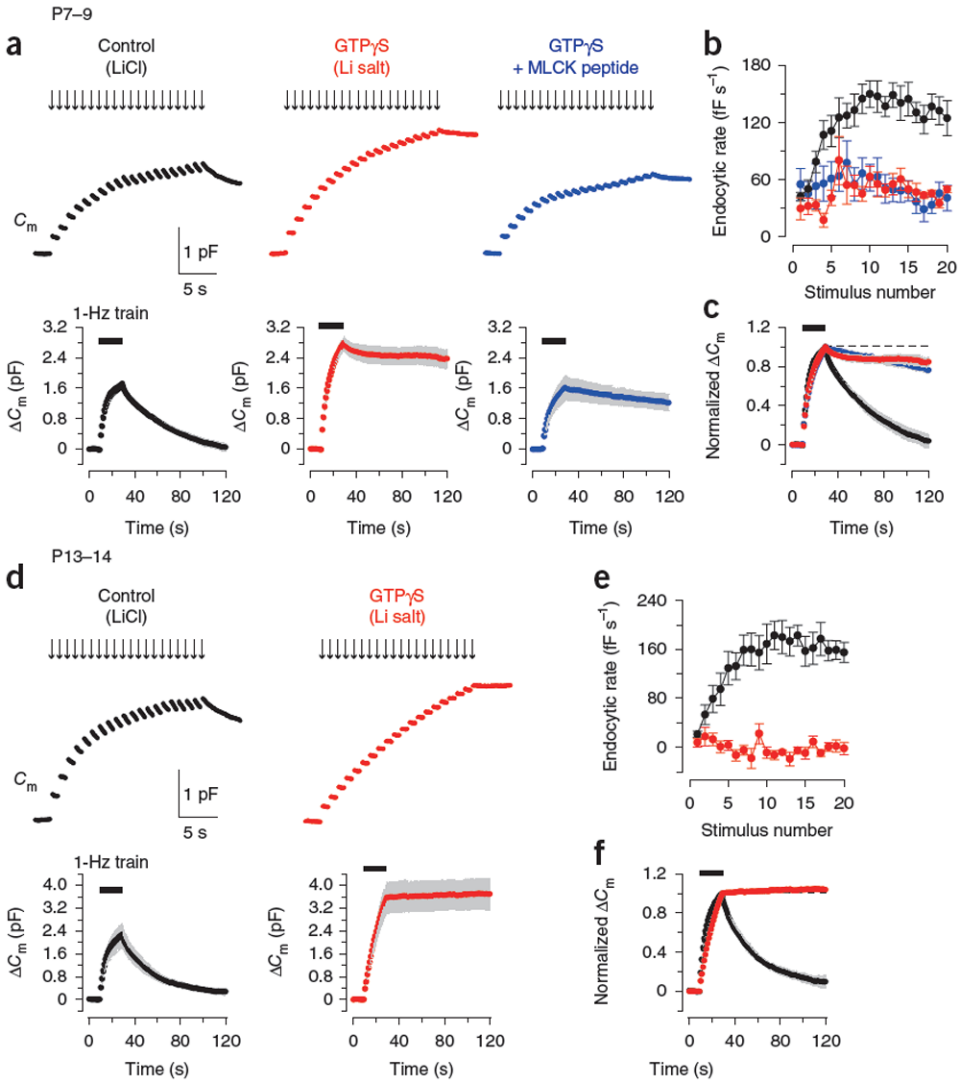

Figure 6.

Developmental decline of GTP-independent endocytic component. (**a**) Top, sample C_m changes induced by a train of 20 depolarizing pulses, with low-[ATP] pipette solution containing 20 mM LiCl (control, with 1 mM GTP, black), 5 mM GTPγS (tetralithium salt, red) or 5 mM GTPγS and 0.2 μM MLCK peptide (blue) at P7–9 calyces. Each depolarizing pulse (from −80 to +10 mV for 20 ms) was preceded by a pre-pulse (stepping to +80 mV for 5 ms) to relieve Ca^{2+} currents from trimeric G protein–dependent inhibition by GTPγS. Bottom, averaged C_m records from the calyces loaded with LiCl (black, $n = 6$), GTPγS (red, $n = 5$) or GTPγS and MLCK peptide (blue, $n = 5$) at P7–9 calyces. Gray shading indicates s.e.m. Black bars indicate the period of stimulation. (**b**) Summary data for the C_m decay rate after each pulse during the 1-Hz train in the terminals loaded with LiCl (black, $n = 7$), GTPγS (red, $n = 6$) or GTPγS and MLCK peptide (blue, $n = 6$) in P7–9 rats. (**c**) Data in **a** normalized at the peaks after the train. (**d–f**) Data are presented as in **a–c** from P13–14 calyces ($n = 5$–8). Error bars represent s.e.m.